

Normative theory of visual receptive fields

Tony Lindeberg

Computational Brain Science Lab, Department of Computational Science and Technology,
KTH Royal Institute of Technology, SE-100 44 Stockholm, Sweden. Email: tony@kth.se

Abstract—This article gives an overview of a normative computational theory of visual receptive fields, by which idealized functional models of early spatial, spatio-chromatic and spatio-temporal receptive fields can be derived in an axiomatic way based on structural properties of the environment in combination with assumptions about the internal structure of a vision system to guarantee consistent handling of image representations over multiple spatial and temporal scales. Interestingly, this theory leads to predictions about visual receptive field shapes with qualitatively very good similarity to biological receptive fields measured in the retina, the LGN and the primary visual cortex (V1) of mammals.

I. INTRODUCTION

When light reaches a visual sensor such as the retina, the information necessary to infer properties about the surrounding world is not contained in the measurement of image intensity at a single point, but from the *relations* between intensity values at different points. A main reason for this is that the incoming light constitutes an *indirect* source of information depending on the interaction between geometric and material properties of objects in the surrounding world and on external illumination sources. Another fundamental reason why cues to the surrounding world need to be collected over *regions* in the visual field as opposed to at single image points is that the measurement process by itself requires the accumulation of energy over non-infinitesimal support regions over space and time. Such a region in the visual field for which a visual sensor or and a visual operator responds to visual input or a visual cell responds to visual stimuli is naturally referred to as a *receptive field* (Hubel and Wiesel [1], [2], [3]) (see Figure 1).

If one considers the theoretical and algorithmic problem of designing a vision system that is going to make use of incoming reflected light to infer properties of the surrounding world, one may ask what types of image operations should be performed on the image data. Would any type of image operation be reasonable? Specifically regarding the notion of receptive fields one may ask what types of receptive field profiles would be reasonable? Is it possible to derive a theoretical model of how receptive fields “ought to” respond to visual data?

Initially, such a problem might be regarded as intractable unless the question can be further specified. It is, however, possible to study this problem systematically using approaches that have been developed in the area of computer vision known as *scale-space theory* (Iijima [4]; Witkin [5]; Koenderink [6]; Koenderink and van Doorn [7], [8]; Lindeberg [9], [10], [11], [12]; Florack [13];

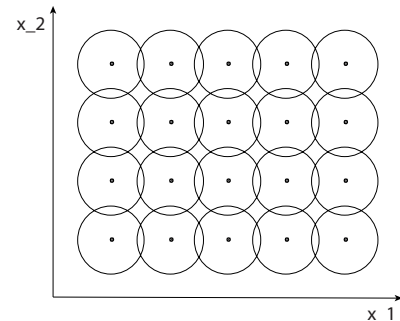


Fig. 1. A receptive field is a region in the visual field for which a visual sensor/neuron/operator responds to visual stimuli. This figure shows a set of partially overlapping receptive fields over the spatial domain with all the receptive fields having the same spatial extent. More generally, one can conceive distributions of receptive fields over space or space-time with the receptive fields of different size, different shape and orientation in space as well as different directions in space-time, where adjacent receptive fields may also have significantly larger relative overlap than shown in this schematic illustration.

Sporring *et al.* [14]; Weickert *et al.* [15]; ter Haar Romeny [16]). A paradigm that has been developed in this field is to impose *structural constraints* on the first stages of visual processing that reflect *symmetry properties* of the environment. Interestingly, it turns out to be possible to substantially reduce the class of permissible image operations from such arguments.

The subject of this article is to describe how structural requirements on the first stages of visual processing as formulated in scale-space theory can be used for deriving idealized functional models of receptive fields and implications of how these theoretical results can be used when modelling biological vision. A main theoretical argument is that idealized functional models for linear receptive fields can be derived *by necessity* given a small set of symmetry requirements that reflect properties of the world that one may naturally require an idealized vision system to be adapted to. In this respect, the treatment bears similarities to approaches in theoretical physics, where symmetry properties are often used as main arguments in the formulation of physical theories of the world. The treatment that will follow will be general in the sense that *spatial, spatio-chromatic and spatio-temporal receptive fields are encompassed by the same unified theory.*

This paper gives a condensed summary of a more general theoretical framework for receptive fields derived and presented in [11], [17], [18], [19] and in turn developed to enable a consistent handling of receptive field responses in terms of provable covariance or invariance properties under natural image transformations (see Figure 2). In

relation to the early publications on this topic [11], [17], [18], this paper presents an improved version of that theory leading to an improved model for the temporal smoothing operation for the specific case of a time-causal image domain [19], where the future cannot be accessed and the receptive fields have to be solely based on information from the present moment and a compact buffer of the past. Specifically, this paper presents the improved axiomatic structure on a compact form more easy to access compared to original publications and also encompassing the better time-causal model.

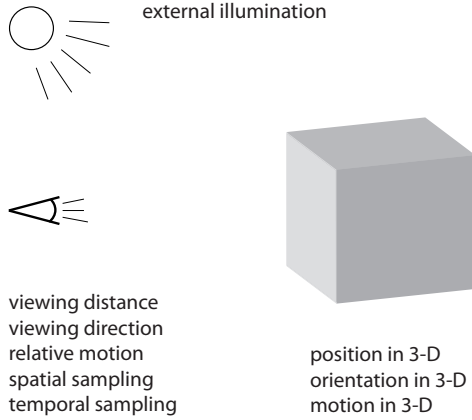


Fig. 2. Basic factors that influence the formation of images for a two-dimensional camera that observes objects in the three-dimensional world. In addition to the position, orientation and motion of the object in 3-D, the perspective projection onto the image plane is affected by the viewing distance, viewing direction and relative motion of the camera in relation to the object, the spatial and temporal sampling characteristics of the image sensor as well the usually unknown external illumination field in relation to the geometry of the scene and the camera.

It will be shown that the presented framework leads to predictions of *receptive field profiles* in good agreement with receptive measurements reported in the literature (Hubel and Wiesel [1], [2], [3]; DeAngelis *et al.* [20], [21]; Conway and Livingstone [22]; Johnson *et al.* [23]). Specifically, explicit phenomenological models will be given of LGN neurons and simple cells in V1 and be compared to related models in terms of Gabor functions (Marčelja [24]; Jones and Palmer [25], [26]; Ringach [27], [28]), differences of Gaussians (Rodieck [29]) or Gaussian derivatives (Koenderink and van Doorn [7]; Young [30]; Young *et al.* [31], [32]). Notably, the evolution properties of the receptive field profiles in this model can be described by diffusion equations and are therefore suitable for implementation on a biological architecture, since the computations can be expressed in terms of communications between neighbouring computational units, where either a single computational unit or a group of computational units may be interpreted as corresponding to a neuron or a group of neurons. Specifically, computational models involving diffusion equations arise in mean field theory for approximating the computations that are performed by populations of neurons (Omurtag *et al.* [33]; Mattia and Guidic [34]; Faugeras *et al.* [35]).

II. STRUCTURAL REQUIREMENTS

In the following, we shall describe a set of structural requirements that can be stated concerning (i) spatial geometry, (ii) spatio-temporal geometry, (iii) the image measurement process with its close relationship to the notion of scale, (iv) internal representations of image data that are to be computed by a general purpose vision system and (v) the parameterization of image intensity with regard to the influence of illumination variations.

A. Static image data over a spatial domain

For time-independent data f over an N -dimensional spatial image domain, we would like to define a family of image representations

$$L(\cdot; s) = \mathcal{T}_s f \quad (1)$$

over a possibly multi-dimensional scale parameter s for some family of image operators \mathcal{T}_s that satisfies:

a) *Linearity and shift-invariance*: To make as few irreversible decisions as possible at the earliest stages, we assume linearity

$$\mathcal{T}_s(a_1 f_1 + a_2 f_2) = a_1 \mathcal{T}_s f_1 + a_2 \mathcal{T}_s f_2. \quad (2)$$

Specifically, this property implies that scale-space properties that we derive for the zero-order image representation L will transfer to any spatial derivative of L .

To ensure that the visual interpretation of an object should be the same irrespective of its position in the image plane, we assume shift invariance

$$\mathcal{T}_s(S_{\Delta x} f) = S_{\Delta x}(\mathcal{T}_s f). \quad (3)$$

Together, the assumptions about linearity and shift-invariance imply that \mathcal{T}_s will be a *convolution* operator.

b) *Semi-group structure over spatial scales*: To ensure that transformations between any pairs of spatial scale levels are of the same form (algebraic closedness), we assume a semi-group structure over spatial scales

$$\mathcal{T}_{s_1} \mathcal{T}_{s_2} = \mathcal{T}_{s_1 + s_2}. \quad (4)$$

c) *Scale covariance under spatial scaling transformations*: Under a uniform scaling transformation of the spatial domain $x' = S_s x$, we assume that spatial scale covariance should hold

$$L'(x'; s') = L(x; s) \Leftrightarrow \mathcal{T}_{S_s(s)} \mathcal{S}_s f = \mathcal{S}_s \mathcal{T}_s f \quad (5)$$

for some transformation $s' = S_s(s)$ of the scale parameter s .

d) *Affine covariance under affine transformations*: Under an affine transformation of the spatial domain $x' = Ax$, we assume that affine covariance should hold

$$L'(x'; s') = L(x; s) \Leftrightarrow \mathcal{T}_{A(s)} \mathcal{A} f = \mathcal{A} \mathcal{T}_s f \quad (6)$$

for some transformation $s' = A(s)$ of the scale parameter.

e) *Non-creation of new structure with increasing scale*: To formalize the requirement that new structures should not be created from finer to coarser scales, we assume *non-enhancement of local extrema*: If at some scale s_0 a point x_0 is a local maximum (minimum) for the mapping $x \mapsto L(x; s_0)$, then (see Figure 3):

- $(\partial_s L)(x; s) \leq 0$ at any spatial maximum,
- $(\partial_s L)(x; s) \geq 0$ at any spatial minimum.

This condition implies a strong condition on the class of possible smoothing kernels $T(\cdot; s)$.

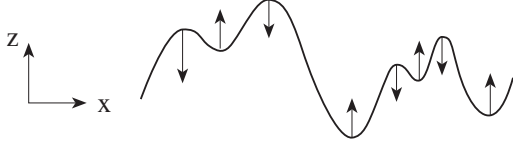


Fig. 3. The requirement of non-enhancement of local extrema is a way of restricting the class of possible image operations by formalizing the notion that new image structures must not be created with increasing scale, by requiring that the value at a local maximum must not increase and that the value at a local minimum must not decrease.

B. Time-dependent image data over space-time

For a time-dependent spatial domain, we do first inherit the structural properties regarding a spatial domain and complement the spatial scale parameter s by a temporal scale parameter τ . In addition, we assume:

f) *Scale covariance under temporal scaling transformations*: Under a scaling transformation of the temporal domain $t' = S_\tau t$, we assume that temporal scale covariance should hold

$$L'(x', t'; s', \tau') = L(x, t; s, \tau) \Leftrightarrow \mathcal{T}_{S_{(s,\tau)}(\tau)} \mathcal{S}_\tau f = \mathcal{S}_\tau \mathcal{T}_{s,\tau} f \quad (7)$$

for some transformation $S_\tau(\tau)$ of the temporal scale parameter τ .

g) *Galilean covariance under Galilean transformations*: To guarantee a consistent visual interpretation under different relative motions between the object and the observer as modelled by Galilean transformations

$$f' = \mathcal{G} f \Leftrightarrow f'(x', t') = f(x, t) \quad \text{with} \quad x' = x + vt, \quad (8)$$

we assume that

$$L'(x', t'; s', \tau') = L(x, t; s, \tau) \Leftrightarrow \mathcal{T}_{G_v(s,\tau)} \mathcal{G}_v f = \mathcal{G}_v \mathcal{T}_{s,\tau} f \quad (9)$$

should hold for some transformation $G_v(s, \tau)$ of the spatio-temporal scale parameters (s, τ) .

h) *Semi-group structure over temporal scales in the case of a non-causal temporal domain*: To ensure that transformations between any pairs of spatial scale levels are of the same form (algebraic closedness), we assume a semi-group structure over temporal scales

$$\mathcal{T}_{\tau_1} \mathcal{T}_{\tau_2} = \mathcal{T}_{\tau_1 + \tau_2}. \quad (10)$$

i) *Cascade structure over temporal scales in the case of a time-causal temporal domain*: Since it can be shown that the assumption of a semi-group structure over temporal scales leads to undesirable temporal dynamics in terms of e.g. longer temporal delays for a time-causal temporal domain [36, Appendix A], we do for a time-causal temporal domain instead assume a weaker cascade smoothing property over temporal scales for the temporal smoothing kernel over temporal scales

$$L(\cdot; \tau_2) = h(\cdot; \tau_1 \mapsto \tau_2) * L(\cdot; \tau_1), \quad (11)$$

where the temporal kernels $h(t; \tau)$ should for any triplets of temporal scale values and temporal delays τ_1, τ_2 and τ_3 obey the transitive property

$$h(\cdot; \tau_1 \mapsto \tau_2) * h(\cdot; \tau_2 \mapsto \tau_3) = h(\cdot; \tau_1 \mapsto \tau_3). \quad (12)$$

j) *Non-enhancement of local space-time extrema in the case of a non-causal temporal domain*: In the case of a non-causal temporal domain, to formalize the requirement that new structures should not be created from finer to coarser spatio-temporal scales, we assume *non-enhancement of local extrema*: If at some scale (s_0, τ_0) a point (x_0, t_0) is a local maximum (minimum) for the mapping $(x, t) \mapsto L(x, t; s_0, \tau_0)$, then

- $\alpha (\partial_s L)(x, t; s, \tau) + \beta (\partial_\tau L)(x, t; s, \tau) \leq 0$ at any spatio-temporal maximum
- $\alpha (\partial_s L)(x, t; s, \tau) + \beta (\partial_\tau L)(x, t; s, \tau) \geq 0$ at any spatio-temporal minimum

should hold in any positive spatio-temporal direction defined from any non-negative linear combinations of α and β . This condition implies a strong condition on the class of possible smoothing kernels $T(\cdot, \cdot; s, \tau)$.

k) *Non-creation of new local extrema or zero-crossings for a purely temporal signal in the case of a non-causal temporal domain*: In the case of a time-causal temporal domain, we do instead require that for a purely temporal signal $f(t)$, the transformation from a finer temporal scale τ_1 to a coarser temporal scale τ_2 must not increase the number of local extrema or zero-crossings in the signal.

III. IDEALIZED RECEPTIVE FIELD FAMILIES

A. Spatial image domain

Based on the above assumptions in Section II-A, it can be shown [11] that when complemented with certain regularity assumptions in terms of Sobolev norms, they imply that spatial scale-space representation L as determined by these must satisfy a diffusion equation of the form

$$\partial_s L = \frac{1}{2} \nabla^T (\Sigma_0 \nabla L) - \delta_0^T \nabla L \quad (13)$$

for some positive semi-definite covariance matrix Σ_0 and some translation vector δ_0 . In terms of convolution kernels, this corresponds to Gaussian kernels of the form

$$g(x; \Sigma_s, \delta_s) = \frac{1}{(2\pi)^{N/2} \sqrt{\det \Sigma_s}} e^{-(x-\delta_s)^T \Sigma_s^{-1} (x-\delta_s)/2}, \quad (14)$$

which for a given $\Sigma_s = s \Sigma_0$ and a given $\delta_s = s \delta_0$ satisfy (13). If we additionally require these kernels to

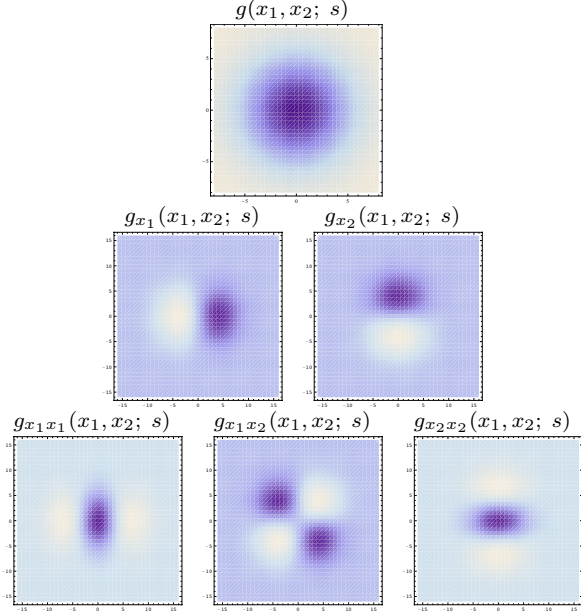


Fig. 4. Spatial receptive fields formed by the 2-D Gaussian kernel with its partial derivatives up to order two. The corresponding family of receptive fields is closed under translations, rotations and scaling transformations, meaning that if the underlying image is subject to a set of such image transformations then it will always be possible to find some possibly other receptive field such that the receptive field responses of the original image and the transformed image can be matched.

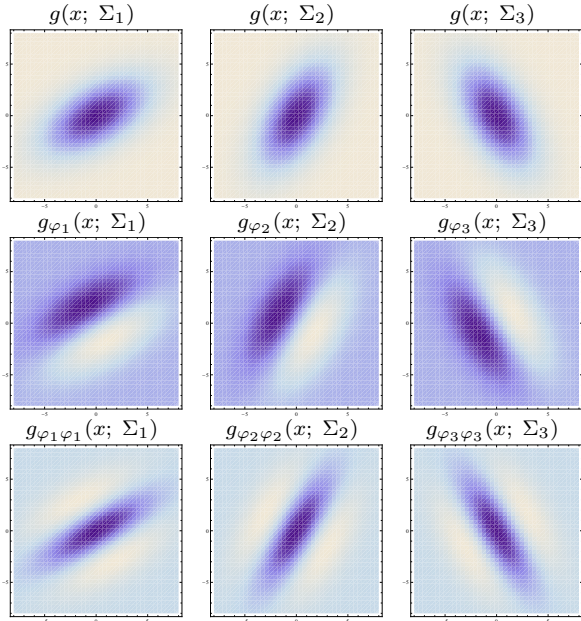


Fig. 5. Spatial receptive fields formed by affine Gaussian kernels and directional derivatives of these, here using three different covariance matrices Σ_1 , Σ_2 and Σ_3 corresponding to the directions $\theta_1 = \pi/6$, $\theta_2 = \pi/3$ and $\theta_3 = 2\pi/3$ of the major eigendirection of the covariance matrix and with first- and second-order directional derivatives computed in the corresponding orthogonal directions φ_1 , φ_2 and φ_3 . The corresponding family of receptive fields is closed under general affine transformations of the spatial domain, including translations, rotations, scaling transformations and perspective foreshortening (although this figure only illustrates variabilities in the orientation of the filter, thereby disregarding variations in both size and degree of elongation).

be mirror symmetric through the origin, then we obtain *affine Gaussian kernels*

$$g(x; \Sigma) = \frac{1}{(2\pi)^{N/2} \sqrt{\det \Sigma}} e^{-x^T \Sigma^{-1} x/2}. \quad (15)$$

Their spatial derivatives constitute a canonical family for expressing receptive fields over a spatial domain that can be summarized on the form

$$T(x; s, \Sigma) = g(x; s\Sigma). \quad (16)$$

Incorporating also the fact that spatial derivatives of these kernels are also compatible with the assumptions underlying this theory, this does specifically for the case of a two-dimensional image domain this lead to spatial receptive fields of the form

$$T_{\varphi^{m_1} \perp \varphi^{m_2}}(x_1, x_2; s, \Sigma) = \partial_{\varphi}^{m_1} \partial_{\perp \varphi}^{m_2} (g(x_1, x_2; s\Sigma)), \quad (17)$$

where

- $x = (x_1, x_2)$ denote the spatial coordinates,
- s denotes the spatial scale,
- Σ denotes a spatial covariance matrix determining the shape of a spatial affine Gaussian kernel,
- m_1 and m_2 denote orders of spatial differentiation,
- $\partial_{\varphi} = \cos \varphi \partial_{x_1} + \sin \varphi \partial_{x_2}$, $\partial_{\perp \varphi} = \sin \varphi \partial_{x_1} - \cos \varphi \partial_{x_2}$ denote spatial directional derivative operators in two orthogonal directions φ and $\perp \varphi$,
- $g(x; s, \Sigma) = \frac{1}{2\pi s \sqrt{\det \Sigma}} e^{-x^T \Sigma^{-1} x/2s}$ is an affine Gaussian kernel with its size determined by the spatial scale parameter s and its shape by the spatial covariance matrix Σ and

Figure 4 and Figure 5 show examples of spatial receptive fields from this family up to second order of spatial

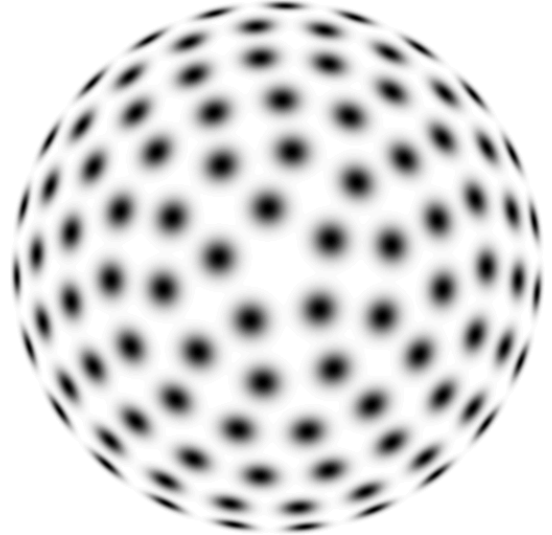


Fig. 6. Distribution of affine Gaussian receptive fields corresponding to a uniform distribution on a hemisphere regarding zero-order smoothing kernels. In the most idealized version of the theory, one can think of all affine receptive fields with their directional derivatives in preferred directions aligned to the eigendirections of the covariance matrix Σ as being present at any position in the image domain. When restricted to a limited number of receptive fields in an actual implementation, there is also an issue of distributing a fixed number of receptive fields over the spatial coordinates $x = (x_1, x_2)$ and the filter parameters Σ .

differentiation. In the most idealized version of the theory, one should think of receptive fields for all combinations of filter parameters as being present at every image point, as illustrated in Figure 6 concerning affine Gaussian receptive fields over different orientations in image space and different eccentricities.

B. Spatio-temporal image domain

Over a non-causal spatio-temporal domain, corresponding arguments as in Section III-A lead to a similar form of diffusion equation as in Equation (13), while expressed over the joint space-time domain $p = (x, t)$ and with δ_0 interpreted as a local drift velocity. After splitting the composed affine Gaussian spatio-temporal smoothing kernel corresponding to (14) while expressed over the joint space-time domain into separate smoothing operations over space and time, this leads to zero-order spatio-temporal receptive fields of the form

$$T(x_1, x_2, t; s, \tau; v, \Sigma) = g(x_1 - v_1 t, x_2 - v_2 t; s, \Sigma) h(t; \tau) \quad (18)$$

After combining that result with the results from corresponding theoretical analysis for a time-causal spatio-temporal domain in [11], [19], the resulting spatio-temporal derivative kernels constituting the spatio-temporal extension of the spatial receptive field model (17) can be reparametrised and summarized on the following form (see [11], [17], [18], [19]):

$$\begin{aligned} T_{\varphi^{m_1 \perp} \varphi^{m_2 \bar{t}^n}}(x_1, x_2, t; s, \tau; v, \Sigma) \\ = \partial_{\varphi}^{m_1} \partial_{\perp \varphi}^{m_2} \partial_{\bar{t}}^n (g(x_1 - v_1 t, x_2 - v_2 t; s, \Sigma) h(t; \tau)) \end{aligned} \quad (19)$$

where

- $x = (x_1, x_2)$ denote the spatial coordinates,
- t denotes time,
- s denotes the spatial scale,
- τ denotes the temporal scale,
- $v = (v_1, v_2)^T$ denotes a local image velocity,
- Σ denotes a spatial covariance matrix determining the shape of a spatial affine Gaussian kernel,
- m_1 and m_2 denote orders of spatial differentiation,
- n denotes the order of temporal differentiation,
- $\partial_{\varphi} = \cos \varphi \partial_{x_1} + \sin \varphi \partial_{x_2}$ and $\partial_{\perp \varphi} = \sin \varphi \partial_{x_1} - \cos \varphi \partial_{x_2}$ denote spatial directional derivative operators in two orthogonal directions φ and $\perp \varphi$,
- $\partial_{\bar{t}} = v_1 \partial_{x_1} + v_2 \partial_{x_2} + \partial_t$ is a velocity-adapted temporal derivative operator aligned to the direction of the local image velocity $v = (v_1, v_2)^T$,
- $g(x; s, \Sigma) = \frac{1}{2\pi s \sqrt{\det \Sigma}} e^{-x^T \Sigma^{-1} x / 2s}$ is an affine Gaussian kernel with its size determined by the spatial scale parameter s and its shape determined by the spatial covariance matrix Σ ,
- $g(x_1 - v_1 t, x_2 - v_2 t; s, \Sigma)$ denotes a spatial affine Gaussian kernel that moves with image velocity $v = (v_1, v_2)$ in space-time and
- $h(t; \tau)$ is a temporal smoothing kernel over time corresponding to a Gaussian kernel $h(t; \tau) = g(t; \tau) = 1/\sqrt{2\pi\tau} \exp(-t^2/2\tau)$ in the case of non-causal time or a cascade of first-order integrators or

equivalently truncated exponential kernels coupled in cascade $h(t; \tau) = h_{composed}(\cdot; \mu)$ according to (21) over a time-causal temporal domain.

This family of spatio-temporal scale-space kernels can be seen as a canonical family of linear receptive fields over a spatio-temporal domain.

For the case of a time-causal temporal domain, the result states that truncated exponential kernels of the form

$$h_{exp}(t; \mu_k) = \begin{cases} \frac{1}{\mu_k} e^{-t/\mu_k} & t \geq 0, \\ 0 & t < 0. \end{cases} \quad (20)$$

coupled in cascade constitute the natural temporal smoothing kernels and leading to a composed convolution kernel of the form

$$h_{composed}(\cdot; \mu) = *_{k=1}^K h_{exp}(\cdot; \mu_k) \quad (21)$$

and corresponding to a set of first-order integrators coupled in cascade (see Figure 7).

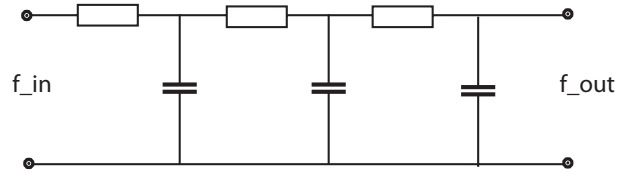


Fig. 7. Electric wiring diagram consisting of a set of resistors and capacitors that emulate a series of first-order integrators coupled in cascade, if we regard the time-varying voltage f_{in} as representing the time varying input signal and the resulting output voltage f_{out} as representing the time varying output signal at a coarser temporal scale. According to the theory of temporal scale-space kernels for one-dimensional signals (Lindeberg [37], [19]; Lindeberg and Fagerström [38]), the corresponding equivalent truncated exponential kernels are the only primitive temporal smoothing kernels that guarantee both temporal causality and non-creation of local extrema (alternatively zero-crossings) with increasing temporal scale.

Two natural ways of distributing the discrete time constants μ_k over temporal scales are studied in detail in [19], [36] corresponding to either a uniform or a logarithmic distribution in terms of the composed variance

$$\tau_K = \sum_{k=1}^K \mu_k^2. \quad (22)$$

Specifically, it is shown in [19] that in the case of a logarithmic distribution of the discrete temporal scale levels, it is possible to consider an infinite number of temporal scale levels that cluster infinitely dense near zero temporal scale

$$\dots \frac{\tau_0}{c^6}, \frac{\tau_0}{c^4}, \frac{\tau_0}{c^2}, \tau_0, c^2 \tau_0, c^4 \tau_0, c^6 \tau_0, \dots \quad (23)$$

so that a *scale-invariant time-causal limit kernel* $\hat{\Psi}(t; \tau, c)$ can be defined obeying self-similarity and scale covariance over temporal scales and with a Fourier transform of the form

$$\hat{\Psi}(\omega; \tau, c) = \prod_{k=1}^{\infty} \frac{1}{1 + i c^{-k} \sqrt{c^2 - 1} \sqrt{\tau} \omega}. \quad (24)$$

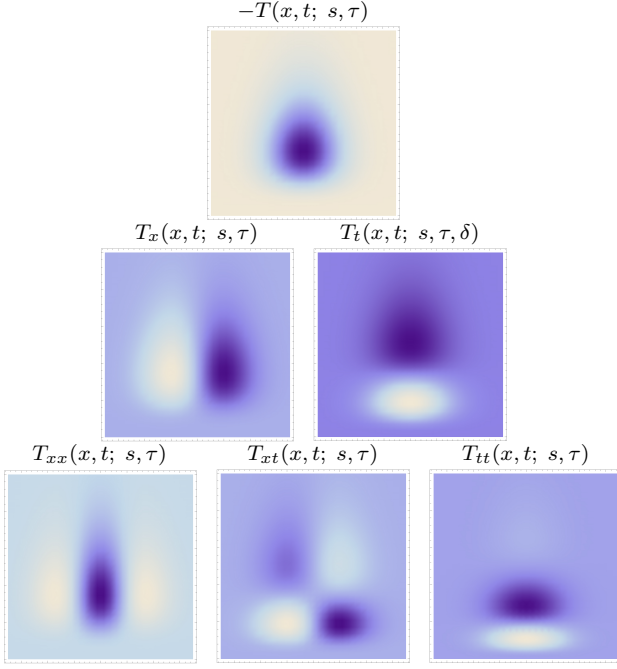


Fig. 8. *Space-time separable kernels* $T_{x^m t^n}(x, t; s, \tau) = \partial_{x^m t^n}(g(x; s)h(t; \tau))$ up to order two obtained as the composition of Gaussian kernels over the spatial domain x and a cascade of truncated exponential kernels over the temporal domain t with a logarithmic distribution of the intermediate temporal scale levels ($s = 1, \tau = 1, K = 7, c = \sqrt{2}$). (Horizontal axis: space x . Vertical axis: time t .)

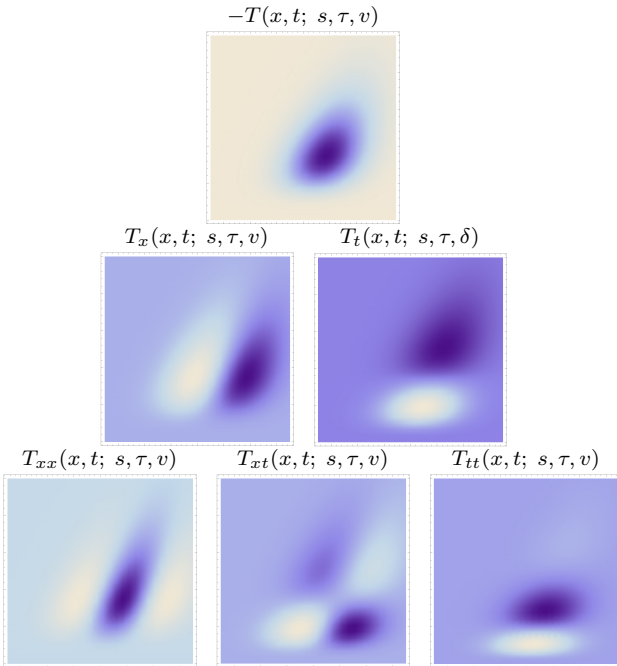


Fig. 9. *Velocity-adapted spatio-temporal kernels* $T_{x^m t^n}(x, t; s, \tau, v) = \partial_{x^m t^n}(g(x - vt; s)h(t; \tau))$ up to order two obtained as the composition of Gaussian kernels over the spatial domain x and a cascade of truncated exponential kernels over the temporal domain t with a logarithmic distribution of the intermediate temporal scale levels ($s = 1, \tau = 1, K = 7, c = \sqrt{2}, v = 0.5$). (Horizontal axis: space x . Vertical axis: time t .)

Figure 8 and Figure 9 show spatio-temporal kernels over a 1+1-dimensional spatio-temporal domain using approximations of the time-causal limit kernel for temporal smoothing over the temporal domain and the Gaussian kernel for spatial smoothing over the spatial domain.

C. Scale normalisation of spatial and spatio-temporal receptive fields

Issues of scale normalisation of the derivative based receptive fields defined from scale-space operations are treated in [39], [40], [41] regarding spatial receptive fields and in [19], [36], [42] regarding spatio-temporal receptive fields.

l) *Scale-normalized spatial receptive fields*: Let s_φ and $s_{\perp\varphi}$ denote the eigenvalues of the composed affine covariance matrix $s\Sigma$ in the spatial receptive field model (17) and let ∂_φ and $\partial_{\perp\varphi}$ denote directional derivative operators along the corresponding eigendirections. Then, the scale-normalized spatial derivative kernel corresponding to the receptive field model (17) is given by

$$T_{\varphi^{m_1} \perp \varphi^{m_2}, norm}(x_1, x_2; s, \Sigma) = s_\varphi^{m_1 \gamma_s / 2} s_{\perp\varphi}^{m_2 \gamma_s / 2} \partial_\varphi^{m_1} \partial_{\perp\varphi}^{m_2} (g(x_1, x_2; s\Sigma)), \quad (25)$$

where γ_s denotes the spatial scale normalization parameter of γ -normalized derivatives and specifically the choice $\gamma_s = 1$ leads to maximum scale invariance in the sense that the magnitude response of the spatial receptive field will be covariant under uniform spatial scaling transformations $(x'_1, x'_2) = (S x_1, S x_2)$, provided that the spatial scale levels are appropriately matched $(s'_\varphi, s'_{\perp\varphi}) = (S^2 s_\varphi, S^2 s_{\perp\varphi})$.

m) *Scale-normalized spatial receptive fields in the case of a non-causal spatio-temporal domain*: For the case of a non-causal spatio-temporal domain, where the temporal smoothing operation in the spatio-temporal receptive field model is performed by a non-causal Gaussian temporal kernel $h(t; \tau) = g(t; \tau) = 1/\sqrt{2\pi\tau} \exp(-t^2/2\tau)$, the scale-normalized spatio-temporal derivative kernel corresponding to the spatio-temporal receptive field model (19) is with corresponding notation regarding the spatial domain as in (25) given by

$$T_{\varphi^{m_1} \perp \varphi^{m_2} \bar{t}^n, norm}(x_1, x_2, t; s, \tau; v, \Sigma) = s_\varphi^{m_1 \gamma_s / 2} s_{\perp\varphi}^{m_2 \gamma_s / 2} \tau^{n \gamma_\tau / 2} \partial_\varphi^{m_1} \partial_{\perp\varphi}^{m_2} \partial_t^n (g(x_1 - v_1 t, x_2 - v_2 t; s, \Sigma) h(t; \tau)) \quad (26)$$

where γ_s and γ_τ denote the spatial and temporal scale normalization parameters of γ -normalized derivatives and specifically the choice $\gamma_s = 1$ and $\gamma_\tau = 1$ leads to maximum scale invariance in the sense that the magnitude response of the spatio-temporal receptive field will be invariant under independent scaling transformations of the spatial and the temporal domains $(x'_1, x'_2, t') = (S_s x_1, S_s x_2, S_\tau t)$, provided that both the spatial and temporal scale levels are appropriately matched $(s'_\varphi, s'_{\perp\varphi}, \tau') = (S_s^2 s_\varphi, S_s^2 s_{\perp\varphi}, S_\tau^2 \tau)$.

n) *Scale-normalized spatial receptive fields in the case of a time-causal spatio-temporal domain*: For the case of a time-causal spatio-temporal domain, where the temporal smoothing operation in the spatio-temporal receptive field model is performed by truncated exponential kernels coupled in cascade $h(t; \tau) = h_{composed}(\cdot; \mu)$, the corresponding scale-normalized spatio-temporal derivative kernel corresponding to the spatio-temporal receptive field model (19) is given by

$$\begin{aligned} T_{\varphi^{m_1} \perp \varphi^{m_2} \bar{t}^n, norm}(x_1, x_2, t; s, \tau; v, \Sigma) \\ = s_{\varphi}^{m_1 \gamma_s / 2} s_{\perp \varphi}^{m_2 \gamma_s / 2} \alpha_{n, \gamma_{\tau}}(\tau) \\ \partial_{\varphi}^{m_1} \partial_{\perp \varphi}^{m_2} \partial_{\bar{t}}^n (g(x_1 - v_1 t, x_2 - v_2 t; s, \Sigma) h(t; \tau)) \end{aligned} \quad (27)$$

where γ_s and γ_{τ} denote the spatial and temporal scale normalization parameters of γ -normalized derivatives and $\alpha_{n, \gamma_{\tau}}(\tau)$ is the temporal scale normalization factor, which for the case of variance-based normalization is given by

$$\alpha_{n, \gamma_{\tau}}(\tau) = \tau^{n \gamma_{\tau} / 2} \quad (28)$$

in agreement with (26) while for the case of L_p -normalization it is given by [19]

$$\alpha_{n, \gamma_{\tau}}(\tau) = \frac{G_{n, \gamma_{\tau}}}{\|h_{t^n}(\cdot; \tau)\|_p} \quad (29)$$

with $G_{n, \gamma_{\tau}}$ denoting the L_p -norm of the n th order scale-normalized derivative of a non-causal Gaussian temporal kernel with scale normalization parameter γ_{τ} . In the specific case when the temporal smoothing is performed using the scale-invariant limit kernel (24), the magnitude response will for the maximally scale invariant choice of scale normalization parameters $\gamma_s = 1$ and $\gamma_{\tau} = 1$ be invariant under independent scaling transformations of the spatial and the temporal domains $(x'_1, x'_2, t') = (S_s x_1, S_s x_2, S_{\tau} t)$ for temporal scaling factors $S_{\tau} = c^j$ that are integer powers of the distribution parameter c of the scale-invariant limit kernel, provided that both the spatial and temporal scale levels are appropriately matched $(s'_{\varphi}, s'_{\perp \varphi}, \tau') = (S_s^2 s_{\varphi}, S_s^2 s_{\perp \varphi}, S_{\tau}^2 \tau)$.

D. Invariance to local multiplicative illumination variations or variations in exposure parameters

The treatment so far has been concerned with modelling receptive fields under natural geometric image transformations, modelled as local scaling transformations, local affine transformations and local Galilean transformations representing the essential dimensions in the variability of a local linearization of the perspective mapping from a surface patch in the world to the image plane or to the tangent plane of the image sphere.

To obtain theoretically well-founded handling of image data under illumination variations, it is natural to represent the image data on a logarithmic luminosity scale

$$f(x, y, t) \sim \log I(x, y, t). \quad (30)$$

Specifically, receptive field responses that are computed from such a logarithmic parameterization of the image

luminosities can be *interpreted physically* as a superposition of relative variations of surface structure and illumination variations. Let us assume a (i) perspective camera model extended with (ii) a thin circular lens for gathering incoming light from different directions and (iii) a Lambertian illumination model extended with (iv) a spatially varying albedo factor for modelling the light that is reflects from surface patterns in the world. Then, it can be shown [17, section 2.3] that a spatio-temporal receptive field response

$$L_{\varphi^{m_1} \perp \varphi^{m_2} \bar{t}^n}(\cdot, \cdot; s, \tau) = \partial_{\varphi^{m_1} \perp \varphi^{m_2} \bar{t}^n} \mathcal{T}_{s, \tau} f(\cdot, \cdot) \quad (31)$$

of the image data f , where $\mathcal{T}_{s, \tau}$ represents the spatio-temporal smoothing operator (here corresponding to a spatio-temporal smoothing kernel of the form (19)) can be expressed as

$$\begin{aligned} L_{\varphi^{m_1} \perp \varphi^{m_2} \bar{t}^n}(x_1, x_2, t; s, \tau) = \\ = \partial_{\varphi^{m_1} \perp \varphi^{m_2} \bar{t}^n} \mathcal{T}_{s, \tau} \left(\log \rho(x, y, t) + \log i(x, y, t) \right. \\ \left. + \log C_{cam}(\tilde{f}(t)) + V(x, y) \right) \end{aligned} \quad (32)$$

where

- (i) $\rho(x, y, t)$ is a spatially dependent *albedo factor* that reflects *properties of surfaces of objects* in the environment with the implicit understanding that this entity may in general refer to points on different surfaces in the world depending on the viewing direction and thus the (possibly time-dependent) image position $(x(t), y(t))$,
- (ii) $i(x, y, t)$ denotes a spatially dependent *illumination field* with the implicit understanding that the amount of incoming light on different surfaces may be different for different points in the world as mapped to corresponding image coordinates (x, y) over time t ,
- (iii) $C_{cam}(\tilde{f}(t)) = \frac{\pi d}{4 f}$ represents the possibly time-dependent *internal camera parameters* with the ratio $\tilde{f} = f/d$ referred to as the *effective f-number*, where d denotes the diameter of the lens and f the focal distance and
- (iv) $V(x, y) = -2 \log(1+x^2+y^2)$ represents a geometric *natural vignetting* effect corresponding to the factor $\log \cos^4(\phi)$ for a planar image plane, with ϕ denoting the angle between the viewing direction (x, y, f) and the surface normal $(0, 0, 1)$ of the image plane. This vignetting term disappears for a spherical camera model.

From the structure of Equation (32) we can note that for any non-zero order of spatial differentiation $(m_1, m_2) > 0$, the influence of the internal camera parameters in $C_{cam}(\tilde{f}(t))$ will disappear because of the spatial differentiation with respect to x or y , and so will the effects of any other multiplicative exposure control mechanism. Furthermore, for any multiplicative illumination variation $i'(x, y) = C i(x, y)$, where C is a scalar constant, the logarithmic luminosity will be transformed as $\log i'(x, y) = \log C + \log i(x, y)$, which implies that the dependency on C will disappear after spatial or temporal differentiation.

Thus, given that the image measurements are performed on a logarithmic brightness scale, the spatio-temporal receptive field responses will be automatically invariant under local multiplicative illumination variations as well as under local multiplicative variations in the exposure parameters of the camera/the eye.

IV. COMPUTATIONAL MODELLING OF BIOLOGICAL RECEPTIVE FIELDS

In two comprehensive reviews, DeAngelis *et al.* [20], [21] present overviews of spatial and temporal response properties of (classical) receptive fields in the central visual pathways. Specifically, the authors point out the limitations of defining receptive fields in the spatial domain only and emphasize the need to characterize receptive fields in the *joint* space-time domain, to describe how a neuron processes the visual image. Conway and Livingstone [22] and Johnson *et al.* [23] show results of corresponding investigations concerning spatio-chromatic receptive fields.

In the following, we will describe how the above mentioned spatial and spatio-temporal scale-space concepts can be used for modelling the spatial, spatio-chromatic and spatio-temporal response properties of biological receptive fields. Indeed, it will be shown that the Gaussian and time-causal scale-space concepts lead to predictions of receptive field profiles that are qualitatively very similar to *all* the receptive field types presented in (DeAngelis *et al.* [20], [21]) and schematic simplifications of most of the receptive fields shown in (Conway and Livingstone [22]) and (Johnson *et al.* [23]).

A. Spatial and spatio-temporal receptive fields in the LGN

Regarding visual receptive fields in the lateral geniculate nucleus (LGN), DeAngelis *et al.* [20], [21] report that most neurons (i) have approximately circular center-surround organization in the spatial domain and that (ii) most of the receptive fields are separable in space-time. There are two main classes of temporal responses for such cells: (i) a “non-lagged cell” is defined as a cell for which the first temporal lobe is the largest one (Figure 11(left)), whereas (ii) a “lagged cell” is defined as a cell for which the second lobe dominates (Figure 11(right)).

When using a time-causal temporal smoothing kernel, the first peak of a first-order temporal derivative will be strongest, whereas second peak of a second-order temporal derivative will be strongest (see [19, Figure 2]). Thus, according to this theory, non-lagged LGN cells can be seen as corresponding to first-order time-causal temporal derivatives, whereas lagged LGN cells can be seen as corresponding to second-order time-causal temporal derivatives.

The spatial response, on the other hand, shows a high similarity to a Laplacian of a Gaussian, leading to an idealized receptive field model of the form (Lindeberg

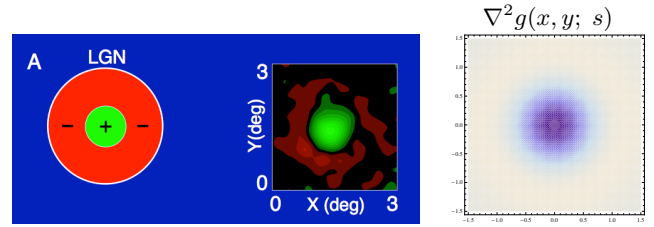


Fig. 10. Spatial component of receptive fields in the LGN. (left) Receptive fields in the LGN have approximately circular center-surround responses in the spatial domain, as reported by DeAngelis *et al.* [20]. (right) In terms of Gaussian derivatives, this spatial response profile can be modelled by the Laplacian of the Gaussian $\nabla^2 g(x, y; s) = (x^2 + y^2 - 2s)/(2\pi s^3) \exp(-(x^2 + y^2)/2s)$, here with $s = 0.35 \text{ deg}^2$.

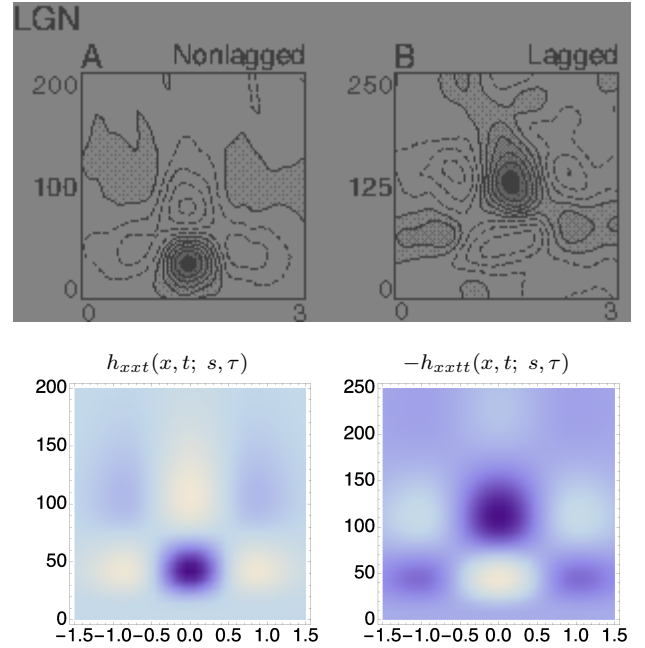


Fig. 11. Computational modelling of space-time separable receptive field profiles in the lateral geniculate nucleus (LGN) as reported by DeAngelis *et al.* [20] using idealized spatio-temporal receptive fields of the form $T(x, t; s, \tau) = \partial_{x^\alpha} \partial_{t^\beta} (g(x, y; s) h(t; \tau))$ according to (19) and with the temporal smoothing function $h(t; \tau)$ modelled as a cascade of first-order integrators/truncated exponential kernels of the form (21). (left) a “non-lagged cell” modelled using first-order temporal derivatives (right) a “lagged cell” modelled using second-order temporal derivatives. Parameter values: (a) h_{xxt} : $\sigma_x = 0.5$ degrees, $\sigma_t = 40$ ms. (b) h_{xxtt} : $\sigma_x = 0.6$ degrees, $\sigma_t = 60$ ms. (Horizontal dimension: space x . Vertical dimension: time t .)

[17, Equation (108)]

$$h_{LGN}(x, y, t; s, \tau) = \pm(\partial_{xx} + \partial_{yy}) g(x, y; s) \partial_{t^n} h(t; \tau). \quad (33)$$

Figure 10 shows a comparison between the spatial component of a receptive field in the LGN with a Laplacian of the Gaussian. This model can also be used for modelling spatial on-center/off-surround and off-center/on-surround receptive fields in the retina. Figure 11 shows results of modelling separable receptive fields in the LGN in this way, using a cascade of truncated exponential kernels of the form (21) for temporal smoothing over the temporal domain.

Regarding the spatial domain, the model

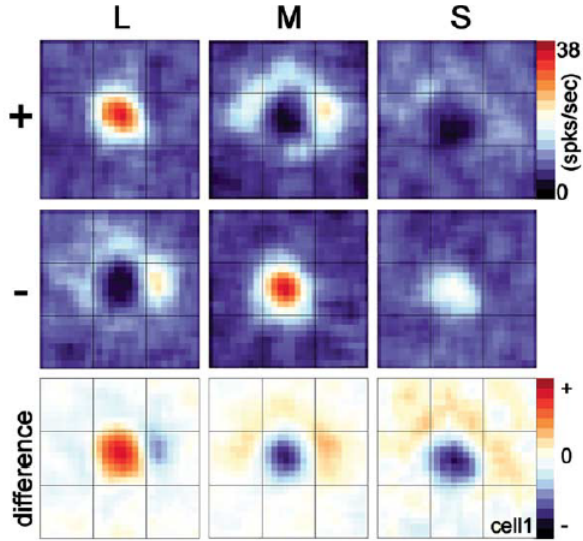


Fig. 12. Spatio-chromatic receptive field response of a *double-opponent neuron* as reported by Conway and Livingstone [22, Figure 2, Page 10831], with the colour channels L, M and S essentially corresponding to red, green and blue, respectively. (From these L, M and S colour channels, corresponding red/green and yellow/blue colour-opponent channels can be formed from the differences between L to M and between L+M to S.)

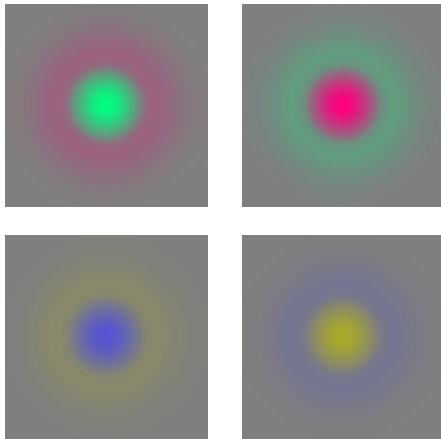


Fig. 13. Spatio-chromatic receptive fields over the spatial domain corresponding to the application of the Laplacian operator to positive and negative red/green and yellow/blue colour opponent channels, respectively. These receptive fields can be seen as idealized models of the spatial component of double-opponent spatio-chromatic receptive fields in the LGN.

in terms of spatial Laplacians of Gaussians ($\partial_{x_1 x_1} + \partial_{x_2 x_2}$) $g(x_1, x_2; s)$ is closely related to differences of Gaussians, which have previously been shown to constitute a good approximation of the spatial variation of receptive fields in the retina and the LGN (Rodieck [29]). This property follows from the fact that the rotationally symmetric Gaussian satisfies the isotropic

diffusion equation

$$\begin{aligned} \frac{1}{2} \nabla^2 L(x; t) &= \partial_t L(x; t) \\ &\approx \frac{L(x; t + \Delta t) - L(x; t)}{\Delta t} \\ &= \frac{DOG(x; t, \Delta t)}{\Delta t} \end{aligned} \quad (34)$$

which implies that differences of Gaussians can be interpreted as approximations of derivatives over scale and hence to Laplacian responses. Conceptually, this implies very good agreement with the spatial component of the LGN model (33) in terms of Laplacians of Gaussians. More recently, Bonin *et al.* [43] have found that LGN responses in cats are well described by difference-of-Gaussians and temporal smoothing complemented by a non-linear contrast gain control mechanism (not modelled here).

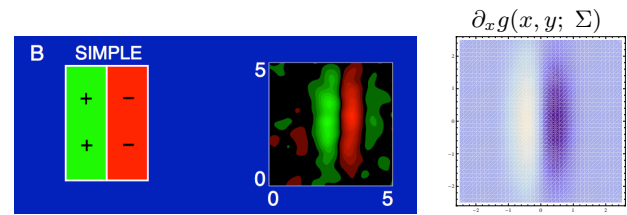


Fig. 14. Example of a receptive field profile over the spatial domain in the primary visual cortex (V1) as reported by DeAngelis *et al.* [20], [21]. (middle) Receptive field profile of a simple cell over image intensities as reconstructed from cell recordings, with positive weights represented as green and negative weights by red. (left) Stylized simplification of the receptive field shape. (right) Idealized model of the receptive field from a first-order directional derivative of an affine Gaussian kernel $\partial_x g(x, y; \Sigma) = \partial_x g(x, y; \lambda_x, \lambda_y)$ according to (15), here with $\lambda_x = 0.2$ and $\lambda_y = 2$ in units of degrees of visual angle, and with positive weights with respect to image intensities represented by white and negative values by violet.

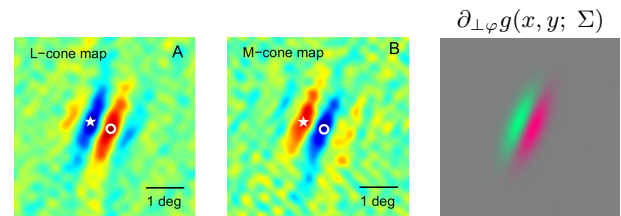


Fig. 15. Example of a colour-opponent receptive field profile over the spatial domain for a double-opponent simple cell in the primary visual cortex (V1) as measured by Johnson *et al.* [23]. (left) Responses to L-cones corresponding to long wavelength red cones, with positive weights represented by red and negative weights by blue. (middle) Responses to M-cones corresponding to medium wavelength green cones, with positive weights represented by red and negative weights by blue. (right) Idealized model of the receptive field from a first-order directional derivative of an affine Gaussian kernel $\partial_{\perp \varphi} g(x, y; \Sigma)$ according to (15) over a red-green colour-opponent channel for $\sigma_1 = \sqrt{\lambda_1} = 0.6$, $\sigma_2 = \sqrt{\lambda_2} = 0.2$ in units of degrees of visual angle, $\alpha = 67$ degrees and with positive weights for the red-green colour-opponent channel represented by red and negative values by green.

B. Double-opponent spatio-chromatic receptive fields in the LGN

In a study of spatio-chromatic response properties of V1 neurons in the alert macaque monkey, Conway

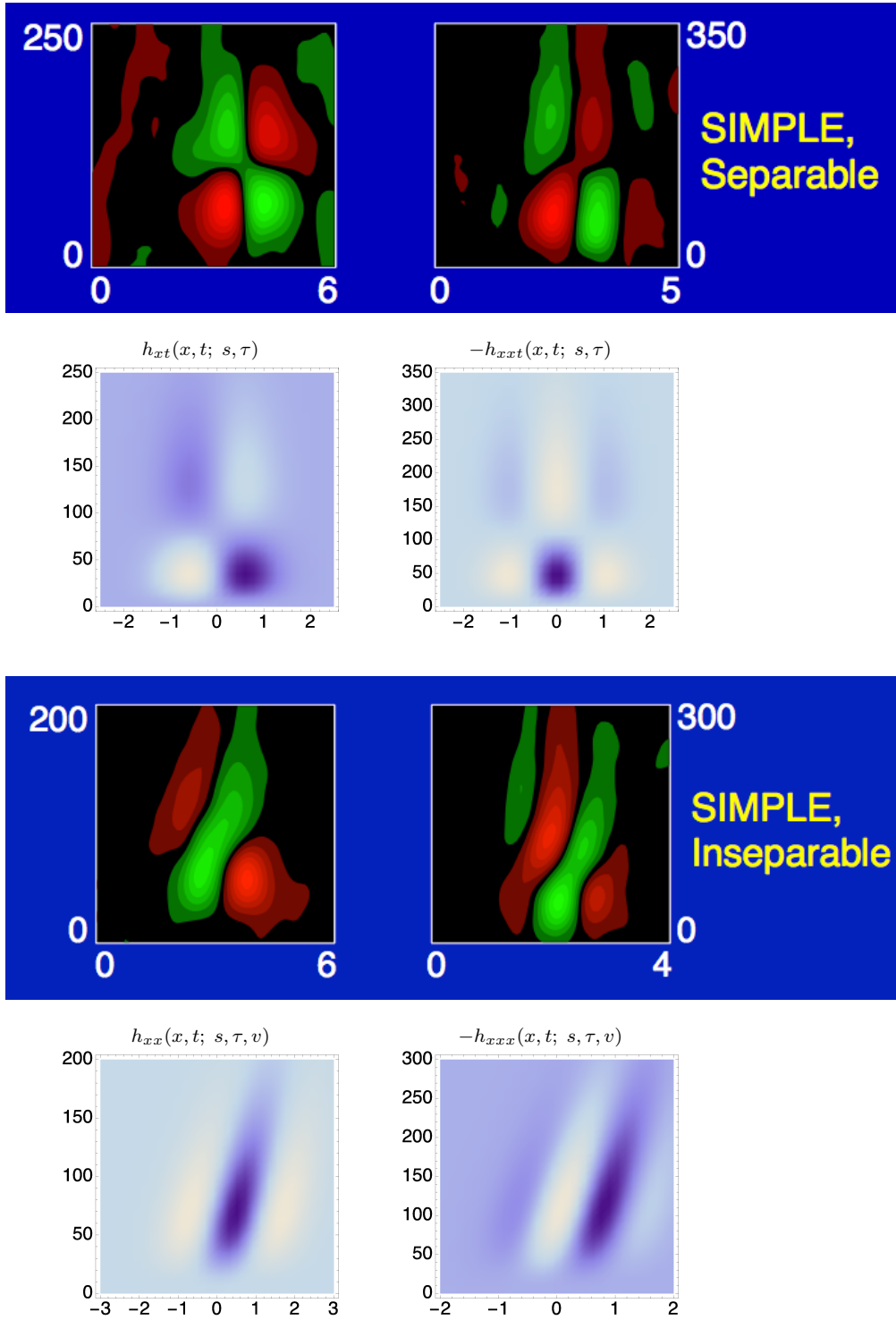


Fig. 16. Computational modelling of simple cells in the primary visual cortex (V1) as reported by DeAngelis *et al.* [20] using idealized spatio-temporal receptive fields of the form $T(x, t; s, \tau, v) = \partial_{x^\alpha} \partial_{t^\beta} g(x - vt; s) h(t; \tau)$ according to Equation (18) and with the temporal smoothing function $h(t; \tau)$ modelled as a cascade of first-order integrators/truncated exponential kernels of the form (21). (left column) Separable receptive fields corresponding to mixed derivatives of first- or second-order derivatives over space with first-order derivatives over time. (right column) Inseparable velocity-adapted receptive fields corresponding to second- or third-order derivatives over space. Parameter values: (a) h_{xt} : $\sigma_x = 0.6$ degrees, $\sigma_t = 60$ ms. (b) h_{xxt} : $\sigma_x = 0.6$ degrees, $\sigma_t = 80$ ms. (c) h_{xx} : $\sigma_x = 0.7$ degrees, $\sigma_t = 50$ ms, $v = 0.007$ degrees/ms. (d) h_{xxx} : $\sigma_x = 0.5$ degrees, $\sigma_t = 80$ ms, $v = 0.004$ degrees/ms. (Horizontal axis: Space x in degrees of visual angle. Vertical axis: Time t in ms.)

and Livingstone [22] describe receptive fields with approximately circular red/green and yellow/blue colour-opponent response properties over the spatio-chromatic domain, see Figure 12. Such cells are referred to as *double-opponent cells*, since they simultaneously compute both spatial and chromatic opponency. According to Conway and Livingstone [22], this cell type can be regarded as the first layer of spatially opponent colour computations.

If we, motivated by the previous application of Laplacian of Gaussian functions to model rotationally symmetric on-center/off-surround and off-center/on-surround receptive fields in the LGN (33), apply the Laplacian of the Gaussian operator to red/green and yellow/blue colour-opponent channels, respectively, we obtain equivalent spatio-chromatic receptive fields corresponding to red-center/green-surround, green-center/red-surround, yellow-center/blue-surround or blue-center/yellow-surround, respectively, as shown in Figure 13 and corresponding to the following spatial receptive field model applied to the RGB channels

$$h_{\text{double-opponent}}(x_1, x_2; s) = \pm (\partial_{x_1 x_1} + \partial_{x_2 x_2}) g(x_1, x_2; s) \begin{pmatrix} \frac{1}{2} & -\frac{1}{2} & 0 \\ \frac{1}{2} & \frac{1}{2} & -1 \end{pmatrix}. \quad (35)$$

In this respect, these spatio-chromatic receptive fields can be used as an idealized model for the spatio-chromatic response properties for double-opponent cells.

C. Spatial, spatio-chromatic and spatio-temporal receptive fields in V1

Concerning the neurons in the primary visual cortex (V1), DeAngelis *et al.* [20], [21] describe that their receptive fields are generally different from the receptive fields in the LGN in the sense that they are (i) oriented in the spatial domain and (ii) sensitive to specific stimulus velocities. Cells (iii) for which there are precisely localized “on” and “off” subregions with (iv) spatial summation within each subregion, (v) spatial antagonism between on- and off-subregions and (vi) whose visual responses to stationary or moving spots can be predicted from the spatial subregions are referred to as *simple cells* (Hubel and Wiesel [1], [2], [3]).

Figure 14 shows an example of the spatial dependency of a simple cell that can be well modelled by a first-order affine Gaussian derivative over image intensities. Figure 15 shows corresponding results for a color-opponent receptive field of a simple cell in V1 that can be modelled as a first-order affine Gaussian spatio-chromatic derivative over an R-G colour-opponent channel.

Figure 16 shows the result of modelling the spatio-temporal receptive fields of simple cells in V1 in this way, using the general idealized model of spatio-temporal receptive fields in Equation (19) in combination with a temporal smoothing kernel obtained by coupling a set of truncated exponential kernels in cascade.

As can be seen from these figures, the proposed idealized receptive field models do quite well reproduce

the qualitative shape of the neurophysiologically recorded biological receptive fields.

V. RELATIONS TO PREVIOUS WORK

Young [30] has shown how spatial receptive fields in cats and monkeys can be well modelled by Gaussian derivatives up to order four. Young *et al.* [31], [32] have also shown how spatio-temporal receptive fields can be modelled by Gaussian derivatives over a spatio-temporal domain, corresponding to the Gaussian spatio-temporal concept described here, although with a different type of parameterization; see also [44], [45] for our closely related earlier work. The normative theory for visual receptive fields presented in [11], [17], [18], [19] and here does first of all provide additional theoretical foundation for Young’s spatial modelling work based on Koenderink and van Doorn’s theory [6], [7], and does additionally provide a conceptual extension to a time-causal spatio-temporal domain that takes into explicit account the fact that the future cannot be accessed. Additionally, our model provides a better parameterization of the spatio-temporal receptive field model over a non-causal spatio-temporal domain based on the Gaussian spatio-temporal scale-space concept.

This model or earlier versions of it has in turn been exploited for modelling of biological receptive fields by Lowe [46], May and Georgeson [47], Hesse and Georgeson [48], Georgeson *et al.* [49], Wallis and Georgeson [50], Hansen and Neumann [51], Wang and Spratling [52], Mahmoodi [53], [54] and Pei *et al.* [55].

A. Relations to modelling by Gabor functions

Gabor functions [56]

$$G(x; s, \omega) = e^{-i\omega x} g(x; s), \quad (36)$$

have been frequently used for modelling spatial receptive fields (Marčelja [24]; Jones and Palmer [25], [26]; Ringach [27], [28]) motivated by their property of minimizing the uncertainty relation. This motivation can, however, be questioned on both theoretical and empirical grounds. Stork and Wilson [57] argue that (i) only complex-valued Gabor functions that cannot describe single receptive field minimize the uncertainty relation, (ii) the real functions that minimize this relation are Gaussian derivatives rather than Gabor functions and (iii) comparisons among Gabor and alternative fits to both psychophysical and physiological data have shown that in many cases other functions (including Gaussian derivatives) provide better fits than Gabor functions do.

Conceptually, the ripples of the Gabor functions, which are given by complex sine waves, are related to the ripples of Gaussian derivatives, which are given by Hermite functions. A Gabor function, however, requires the specification of a scale parameter and a frequency, whereas a Gaussian derivative requires a scale parameter and the order of differentiation. With the Gaussian derivative model, receptive fields of different orders can be mutually related by derivative operations, and be computed from each other by nearest-neighbour operations. The zero-order receptive

fields as well as the derivative based receptive fields can be modelled by diffusion equations, and can therefore be implemented by computations between neighbouring computational units.

In relation to invariance properties, the family of affine Gaussian kernels is closed under affine image deformations, whereas the family of Gabor functions obtained by multiplying rotationally symmetric Gaussians with sine and cosine waves is not closed under affine image deformations. This means that it is not possible to compute truly affine invariant image representations from such Gabor functions. Instead, given a pair of images that are related by a non-uniform image deformation, the lack of affine covariance implies that there will be a systematic bias in image representations derived from such Gabor functions, corresponding to the difference between the backprojected Gabor functions in the two image domains. If using receptive profiles defined from directional derivatives of affine Gaussian kernels, it will on the other hand be possible to compute affine invariant image representations, in turn providing better internal consistency between receptive field responses computed from different views of objects in the world.

With regard to invariance to multiplicative illumination variations, the even cosine component of a Gabor function does in general not have its integral equal to zero, which means that the illumination invariant properties under multiplicative illumination variations or exposure control mechanisms described in section III-D do not hold for Gabor functions.

In this respect, the Gaussian derivative model is simpler, it can be related to image measurements by differential geometry, be derived axiomatically from symmetry principles, be computed from a minimal set of connections and allows for provable invariance properties under locally linearized image deformations (affine transformations) as well as local multiplicative illumination variations and exposure control mechanisms.

B. Relations to approaches for learning receptive fields from natural image statistics

Work has also been performed on learning receptive field properties and visual models from the statistics of natural image data (Field [58]; van der Schaaf and van Hateren [59]; Olshausen and Field [60]; Rao and Ballard [61]; Simoncelli and Olshausen [62]; Geisler [63]; Hyvärinen *et al.* [64]; Lörincz [65]) and been shown to lead to the formation of similar receptive fields as found in biological vision. The proposed theory of receptive fields can be seen as describing basic physical constraints under which a learning based method for the development of receptive fields will operate and the solutions to which an optimal adaptive system may converge to, if exposed to a sufficiently large and representative set of natural image data (see Figure 17).

Field [58] as well as Doi and Lewicki [66] have described how "natural images are not random, instead they exhibit statistical regularities" and have used such statistical regularities for constraining the properties of

receptive fields. The theory presented in this paper can be seen as a theory at a higher level of abstraction, in terms of basic principles that reflect properties of the environment that in turn determine properties of the image data, without need for explicitly constructing specific statistical models for the image statistics. Specifically, the proposed theory can be used for explaining why the above mentioned statistical models lead to qualitatively similar types of receptive fields as the idealized functional models of receptive fields obtained from our theory.

An interesting observation that can be made from the similarities between the receptive field families derived by necessity from the assumptions and receptive profiles found by cell recordings in biological vision, is that receptive fields in the retina, LGN and V1 of higher mammals are very close to *ideal* in view of the stated structural requirements/symmetry properties. In this sense, biological vision can be seen as having adapted very well to the transformation properties of the outside world and the transformations that occur when a three-dimensional world is projected to a two-dimensional image domain.

C. Logarithmic brightness scale

The notion of a *logarithmic brightness scale* goes back to the Greek astronomer Hipparchus, who constructed a subjective scale for the brightness of stars in six steps labelled "1 ... 6", where the brightest stars were said to be of the first magnitude ($m = 1$) while the faintest stars near the limits of human perception were of the sixth magnitude. Later, when quantitative physical measurements were made possible of the intensities of different stars, it was noted that Hipparchus subjective scale did indeed correspond to a logarithmic scale. In astronomy today, the *apparent brightness* of stars is still measured on a logarithmic scale, although extended over a much wider span of intensity values. A logarithmic transformation of image intensities is also used in the retinex theory (Land [67], [68]).

In psychophysics, the *Weber-Fechner law* attempts to describe the relationship between the physical magnitude and the perceived intensity of stimuli. This law states that the ratio of an increment threshold ΔI for a just noticeable difference in relation to the background intensity I is constant over large ranges of magnitude variations [69, Pages 671–672]

$$\frac{\Delta I}{I} = k \quad (37)$$

where the constant k is referred to as the Weber ratio. The theoretical analysis of invariance properties of a logarithmic brightness scale under multiplicative transformations of the illumination field as well as multiplicative exposure control mechanisms is in excellent agreement with these psychophysical findings. If one considers an adaptive image exposure mechanism in the retina that adapts the size of the pupil and the sensitivity of the photopigments such that relative range variability in the signal divided by the mean illumination is held constant (37) (see *e.g.* Peli [70]), then such an adaptation mechanism can be seen

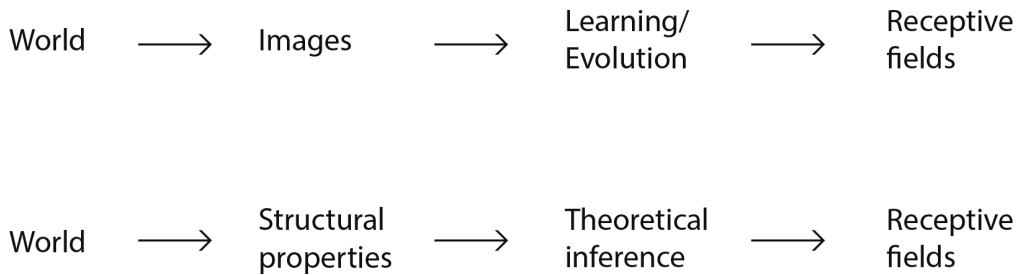


Fig. 17. Two structurally different ways of deriving receptive field shapes for a vision system intended to infer properties of the world by either biological or artificial visual perception. (top row) A traditional model for learning receptive fields shapes consists of collecting real-world image data from the environment, and then applying learning algorithms possibly in combination with evolution over multiple generations of the organism that the vision system is a part of. (bottom row) With the normative theory for receptive fields presented in this paper, a short-cut is made in the sense that the derivation of receptive field shapes starts from structural properties of the world (corresponding to symmetry properties in theoretical physics) from which receptive field shapes are constrained by theoretical mathematical inference.

as implementing an approximation of the derivative of a logarithmic transformation

$$d(\log z) = \frac{dz}{z}. \quad (38)$$

For a strictly positive entity z , there are also information theoretic arguments to regard $\log z$ as a default parameterization (Jaynes [71]). This property is essentially related to the fact that the ratio dz/z then becomes a dimensionless integration measure. A general recommendation of care should, however, be taken when using such reasoning based on dimensionality arguments, since important phenomena could be missed, *e.g.*, in the presence of hidden variables. The physical modelling of the effect on illumination variation on receptive field measurements in section III-D provides a formal justification for using a logarithmic brightness scale in this context as well as an additional contribution of showing how the receptive field measurements can be related to inherent physical properties of object surfaces in the environment.

VI. SUMMARY

Neurophysiological cell recordings have shown that mammalian vision has developed receptive fields that are tuned to different sizes and orientations in the image domain as well as to different image velocities in space-time. A main message of this article has been to show that it is possible to derive such families of receptive field profiles *by necessity*, given a set of structural requirements on the first stages of visual processing as formalized into the notion of an *idealized vision system*, and whose functionality is determined by set of mathematical and physical assumptions (see Figure 17).

These structural requirements reflect *structural properties of the world* for the receptive fields to be compatible with natural image transformations including: (i) variations in the sizes of objects in the world, (ii) variations in the viewing distance, (iii) variations in the viewing direction, (iv) relative motion between objects in the world and the observer, (v) the speed by which temporal events occur and (vi) locally multiplicative illumination variations. which are natural to *adapt to* for a vision system that is to *interact with the world* in a successful

manner. In a competition between different organisms, adaptation to these properties may constitute an *evolutionary advantage*.

The presented theoretical model provides a *normative theory* for deriving *functional models of linear receptive fields* based on Gaussian derivatives and closely related operators. Specifically, the proposed theory can *explain* the different shapes of receptive field profiles that are found in biological vision from a requirement that the visual system should be able to compute covariant receptive field responses under the natural types of image transformations that occur in the environment, to enable the computation of invariant representations for perception at higher levels [18].

The presented theory leads to a computational framework for defining spatial and spatio-temporal receptive fields from visual data with the attractive properties that: (i) the receptive field profiles can be derived *by necessity* from first principles and (ii) it leads to *predictions* about receptive field profiles in good agreement with receptive fields found by cell recordings in biological vision. Specifically, idealized functional models have been presented for space-time separable receptive fields in the retina and the LGN and for both space-time separable and non-separable simple cells in the primary visual cortex (V1).

The qualitatively very good agreement between the predicted receptive field profiles from the normative axiomatic theory indicates that the earliest receptive fields in higher mammal vision have reached a state that can be seen as very close to *ideal* in view of the stated structural requirements/symmetry properties. In this sense, biological vision can be seen as having adapted very well to the transformation properties of the outside world and the transformations that occur when a three-dimensional world is projected onto a two-dimensional image domain.

Compared to more common approaches of learning receptive field profiles from natural image statistics, the proposed framework makes it possible to derive the shapes of idealized receptive fields without any need for training data. The proposed framework for invariance and covariance properties also adds explanatory value by

showing that the families of receptive profiles tuned to different orientations in space and image velocities in space-time that can be observed in biological vision can be explained from the requirement that the receptive fields should be covariant under basic image transformations to enable true invariance properties. If the underlying receptive fields would not be covariant, then there would be a systematic bias in the visual operations, corresponding to the amount of mismatch between the backprojected receptive fields.

Corresponding types of arguments applied to the area of hearing, lead to the formulation of a normative theory of auditory receptive fields (Lindeberg and Friberg [72], [73]).

ACKNOWLEDGMENTS

The support from the Swedish Research Council (Contract No. 2014-4083) is gratefully acknowledged.

REFERENCES

- [1] D. H. Hubel and T. N. Wiesel, "Receptive fields of single neurones in the cat's striate cortex," *J Physiol*, vol. 147, pp. 226–238, 1959.
- [2] —, "Receptive fields, binocular interaction and functional architecture in the cat's visual cortex," *J Physiol*, vol. 160, pp. 106–154, 1962.
- [3] —, *Brain and Visual Perception: The Story of a 25-Year Collaboration*. Oxford University Press, 2005.
- [4] T. Iijima, "Observation theory of two-dimensional visual patterns," Papers of Technical Group on Automata and Automatic Control, IECE, Japan, Tech. Rep., 1962.
- [5] A. P. Witkin, "Scale-space filtering," in *Proc. 8th Int. Joint Conf. Art. Intell.*, Karlsruhe, Germany, Aug. 1983, pp. 1019–1022.
- [6] J. J. Koenderink, "The structure of images," *Biological Cybernetics*, vol. 50, pp. 363–370, 1984.
- [7] J. J. Koenderink and A. J. van Doorn, "Representation of local geometry in the visual system," *Biological Cybernetics*, vol. 55, pp. 367–375, 1987.
- [8] —, "Generic neighborhood operators," *IEEE Trans. Pattern Analysis and Machine Intell.*, vol. 14, no. 6, pp. 597–605, Jun. 1992.
- [9] T. Lindeberg, *Scale-Space Theory in Computer Vision*. Springer, 1993.
- [10] —, "Scale-space theory: A basic tool for analysing structures at different scales," *Journal of Applied Statistics*, vol. 21, no. 2, pp. 225–270, 1994, also available from <http://www.csc.kth.se/~tony/abstracts/Lin94-SI-abstract.html>.
- [11] —, "Generalized Gaussian scale-space axiomatics comprising linear scale-space, affine scale-space and spatio-temporal scale-space," *Journal of Mathematical Imaging and Vision*, vol. 40, no. 1, pp. 36–81, 2011.
- [12] —, "Generalized axiomatic scale-space theory," in *Advances in Imaging and Electron Physics*, P. Hawkes, Ed. Elsevier, 2013, vol. 178, pp. 1–96.
- [13] L. M. J. Florack, *Image Structure*, ser. Series in Mathematical Imaging and Vision. Springer, 1997.
- [14] J. Sporring, M. Nielsen, L. Florack, and P. Johansen, Eds., *Gaussian Scale-Space Theory: Proc. PhD School on Scale-Space Theory*, ser. Series in Mathematical Imaging and Vision. Copenhagen, Denmark: Springer, 1997.
- [15] J. Weickert, S. Ishikawa, and A. Imiya, "Linear scale-space has first been proposed in Japan," *Journal of Mathematical Imaging and Vision*, vol. 10, no. 3, pp. 237–252, 1999.
- [16] B. ter Haar Romeny, *Front-End Vision and Multi-Scale Image Analysis*. Springer, 2003.
- [17] T. Lindeberg, "A computational theory of visual receptive fields," *Biological Cybernetics*, vol. 107, no. 6, pp. 589–635, 2013.
- [18] —, "Invariance of visual operations at the level of receptive fields," *PLOS ONE*, vol. 8, no. 7, p. e66990, 2013.
- [19] —, "Time-causal and time-recursive spatio-temporal receptive fields," *Journal of Mathematical Imaging and Vision*, vol. 55, no. 1, pp. 50–88, 2016.
- [20] G. C. DeAngelis, I. Ohzawa, and R. D. Freeman, "Receptive field dynamics in the central visual pathways," *Trends in Neuroscience*, vol. 18, no. 10, pp. 451–457, 1995.
- [21] G. C. DeAngelis and A. Anzai, "A modern view of the classical receptive field: Linear and non-linear spatio-temporal processing by V1 neurons," in *The Visual Neurosciences*, L. M. Chalupa and J. S. Werner, Eds. MIT Press, 2004, vol. 1, pp. 704–719.
- [22] B. R. Conway and M. S. Livingstone, "Spatial and temporal properties of cone signals in alert macaque primary visual cortex," *Journal of Neuroscience*, vol. 26, no. 42, pp. 10 826–10 846, 2006.
- [23] E. N. Johnson, M. J. Hawken, and R. Shapley, "The orientation selectivity of color-responsive neurons in Macaque V1," *The Journal of Neuroscience*, vol. 28, no. 32, pp. 8096–8106, 2008.
- [24] S. Marcelja, "Mathematical description of the responses of simple cortical cells," *Journal of Optical Society of America*, vol. 70, no. 11, pp. 1297–1300, 1980.
- [25] J. Jones and L. Palmer, "The two-dimensional spatial structure of simple receptive fields in cat striate cortex," *J. of Neurophysiology*, vol. 58, pp. 1187–1211, 1987.
- [26] —, "An evaluation of the two-dimensional Gabor filter model of simple receptive fields in cat striate cortex," *J. of Neurophysiology*, vol. 58, pp. 1233–1258, 1987.
- [27] D. L. Ringach, "Spatial structure and symmetry of simple-cell receptive fields in macaque primary visual cortex," *Journal of Neurophysiology*, vol. 88, pp. 455–463, 2002.
- [28] —, "Mapping receptive fields in primary visual cortex," *Journal of Physiology*, vol. 558, no. 3, pp. 717–728, 2004.
- [29] R. W. Rodieck, "Quantitative analysis of cat retinal ganglion cell response to visual stimuli," *Vision Research*, vol. 5, no. 11, pp. 583–601, 1965.
- [30] R. A. Young, "The Gaussian derivative model for spatial vision: I. Retinal mechanisms," *Spatial Vision*, vol. 2, pp. 273–293, 1987.
- [31] R. A. Young, R. M. Lesperance, and W. W. Meyer, "The Gaussian derivative model for spatio-temporal vision: I. Cortical model," *Spatial Vision*, vol. 14, no. 3, 4, pp. 261–319, 2001.
- [32] R. A. Young and R. M. Lesperance, "The Gaussian derivative model for spatio-temporal vision: II. Cortical data," *Spatial Vision*, vol. 14, no. 3, 4, pp. 321–389, 2001.
- [33] A. Omurtag, B. W. Knight, and L. Sirovich, "On the simulation of large populations of neurons," *Journal of Computational Neuroscience*, vol. 8, pp. 51–63, 2000.
- [34] M. Mattia and P. D. Giudice, "Population dynamics of interacting spiking neurons," *Physics Review E*, vol. 66, no. 5, p. 051917, 2002.
- [35] O. Faugeras, J. Toubol, and B. Cessac, "A constructive mean-field analysis of multi-population neural networks with random synaptic weights and stochastic inputs," *Frontiers in Computational Neuroscience*, vol. 3, no. 1, p. 10.3389/neuro.10.001.2009, 2009.
- [36] T. Lindeberg, "Temporal scale selection in time-causal scale space," *Journal of Mathematical Imaging and Vision*, 2017, doi:10.1007/s10851-016-0691-3.
- [37] —, "Scale-space for discrete signals," *IEEE Trans. Pattern Analysis and Machine Intell.*, vol. 12, no. 3, pp. 234–254, Mar. 1990.
- [38] T. Lindeberg and D. Fagerström, "Scale-space with causal time direction," in *Proc. European Conf. on Computer Vision (ECCV'96)*, ser. Springer LNCS, vol. 1064, Cambridge, UK, Apr. 1996, pp. 229–240.
- [39] T. Lindeberg, "Feature detection with automatic scale selection," *International Journal of Computer Vision*, vol. 30, no. 2, pp. 77–116, 1998.
- [40] —, "Edge detection and ridge detection with automatic scale selection," *International Journal of Computer Vision*, vol. 30, no. 2, pp. 117–154, 1998.
- [41] —, "Scale selection," in *Computer Vision: A Reference Guide*, K. Ikeuchi, Ed. Springer, 2014, pp. 701–713.
- [42] —, "Spatio-temporal scale selection in video data," *In preparation*, 2017.
- [43] V. Bonin, V. Mante, and M. Carandini, "The suppressive field of neurons in the lateral geniculate nucleus," *The Journal of Neuroscience*, vol. 25, no. 47, pp. 10 844–10 856, 2005.
- [44] T. Lindeberg, "Linear spatio-temporal scale-space," in *Proc. International Conference on Scale-Space Theory in Computer Vision (Scale-Space'97)*, ser. Springer LNCS, B. M. ter Haar Romeny, L. M. J. Florack, J. J. Koenderink, and M. A. Viergever, Eds., vol. 1252. Utrecht, The Netherlands: Springer, Jul. 1997, pp. 113–127.

- [45] —, “Linear spatio-temporal scale-space,” Dept. of Numerical Analysis and Computer Science, KTH, Tech. Rep. ISRN KTH/NA/P-01/22--SE, Nov. 2001, available from <http://www.csc.kth.se/cvap/abstracts/cvap257.html>.
- [46] D. G. Lowe, “Towards a computational model for object recognition in IT cortex,” in *Biologically Motivated Computer Vision*, ser. Springer LNCS, vol. 1811. Springer, 2000, pp. 20–31.
- [47] K. A. May and M. A. Georgeson, “Blurred edges look faint, and faint edges look sharp: The effect of a gradient threshold in a multi-scale edge coding model,” *Vision Research*, vol. 47, no. 13, pp. 1705–1720, 2007.
- [48] G. S. Hesse and M. A. Georgeson, “Edges and bars: where do people see features in 1-D images?” *Vision Research*, vol. 45, no. 4, pp. 507–525, 2005.
- [49] M. A. Georgeson, K. A. May, T. C. A. Freeman, and G. S. Hesse, “From filters to features: Scale-space analysis of edge and blur coding in human vision,” *Journal of Vision*, vol. 7, no. 13, pp. 7–, 2007.
- [50] S. A. Wallis and M. A. Georgeson, “Mach edges: Local features predicted by 3rd derivative spatial filtering,” *Vision Research*, vol. 49, no. 14, pp. 1886–1893, 2009.
- [51] T. Hansen and H. Neumann, “A recurrent model of contour integration in primary visual cortex,” *Journal of Vision*, vol. 8, no. 8, pp. 8–, 2008.
- [52] Q. Wang and M. W. Spratling, “Contour detection in colour images using a neurophysiologically inspired model,” *Cognitive Computation*, vol. 8, no. 6, pp. 1027–1035, 2016.
- [53] S. Mahmoodi, “Linear neural circuitry model for visual receptive fields,” *Journal of Mathematical Imaging and Vision*, vol. 54, no. 2, pp. 1–24, 2016.
- [54] —, “Nonlinearity in simple and complex cells in early biological visual systems,” *Journal of Mathematical Imaging and Vision*, pp. 1–10, 2017.
- [55] Z.-J. Pei, G.-X. Gao, B. Hao, Q.-L. Qiao, and H.-J. Ai, “A cascade model of information processing and encoding for retinal prosthesis,” *Neural Regeneration Research*, vol. 11, no. 4, p. 646, 2016.
- [56] D. Gabor, “Theory of communication,” *J. of the IEE*, vol. 93, pp. 429–457, 1946.
- [57] D. G. Stork and H. R. Wilson, “Do Gabor functions provide appropriate descriptions of visual cortical receptive fields,” *Journal of Optical Society of America*, vol. 7, no. 8, pp. 1362–1373, 1990.
- [58] D. J. Field, “Relations between the statistics of natural images and the response properties of cortical cells,” *Journal of Optical Society of America*, vol. 4, pp. 2379–2394, 1987.
- [59] A. van der Schaaf and J. H. van Hateren, “Modelling the power spectra of natural images: Statistics and information,” *Vision Research*, vol. 36, no. 17, pp. 2759–2770, 1996.
- [60] B. A. Olshausen and D. J. Field, “Emergence of simple-cell receptive field properties by learning a sparse code for natural images,” *Journal of Optical Society of America*, vol. 381, pp. 607–609, 1996.
- [61] R. P. N. Rao and D. H. Ballard, “Development of localized oriented receptive fields by learning a translation-invariant code for natural images,” *Computation in Neural Systems*, vol. 9, no. 2, pp. 219–234, 1998.
- [62] E. P. Simoncelli and B. A. Olshausen, “Natural image statistics and neural representations,” *Annual Review of Neuroscience*, vol. 24, pp. 1193–1216, 2001.
- [63] W. S. Geisler, “Visual perception and the statistical properties of natural scenes,” *Annual Review of Psychology*, vol. 59, pp. 10.1–10.26, 2008.
- [64] A. Hyvärinen, J. Hurri, and P. O. Hoyer, *Natural Image Statistics: A Probabilistic Approach to Early Computational Vision*, ser. Computational Imaging and Vision. Springer, 2009.
- [65] A. Lörincz, Z. Palotai, and G. Szirtes, “Efficient sparse coding in early sensory processing: Lessons from signal recovery,” *PLOS Computational Biology*, vol. 8(3), no. e1002372, 2012, 10.1371/journal.pcbi.1002372.
- [66] E. Doi and M. S. Lewicki, “Relations between the statistical regularities of natural images and the response properties of the early visual system,” in *Japanese Cognitive Science Society: Sig P & P*, Kyoto University, 2005, pp. 1–8.
- [67] E. H. Land, “The retinex theory of colour vision,” *Proc. Royal Institution of Great Britain*, vol. 57, pp. 23–58, 1974.
- [68] —, “Recent advances in retinex theory,” *Vision Research*, vol. 26, no. 1, pp. 7–21, 1986.
- [69] S. E. Palmer, *Vision Science: Photons to Phenomenology*. MIT Press, 1999, first Edition.
- [70] E. Peli, “Contrast in complex images,” *Journal of the Optical Society of America (JOSA A)*, vol. 7, no. 10, pp. 2032–2040, 1990.
- [71] E. T. Jaynes, “Prior probabilities,” *Trans. on Systems Science and Cybernetics*, vol. 4, no. 3, pp. 227–241, 1968.
- [72] T. Lindeberg and A. Friberg, “Idealized computational models of auditory receptive fields,” *PLOS ONE*, vol. 10, no. 3, pp. e0119032:1–58, 2015.
- [73] —, “Scale-space theory for auditory signals,” in *Proc. Scale-Space and Variational Methods for Computer Vision (SSVM 2015)*, ser. Lecture Notes in Computer Science, vol. 9087. Springer, 2015, pp. 3–15.